

# Formation of the Supersonic Stellar Wind: Parker's Theory Revisited

Paul Song<sup>1</sup>, Jiannan Tu<sup>1</sup>, Stanley W. H. Cowley<sup>2</sup>, Chi Wang<sup>3</sup>, Hui Li<sup>3</sup>

<sup>1</sup>Space Science Laboratory and Department of Physics, University of Massachusetts Lowell,  
Lowell, MA 01854, USA

<sup>2</sup>Department of Physics and Astronomy, University of Leicester, Leicester, UK

<sup>3</sup>National Space Science Center, Chinese Academy of Sciences,  
Beijing 100190, China

## Abstract

We examine and propose to fundamentally modify the classical theory of stellar wind formation. To form a supersonic stellar wind, the classical theory requires that a subsonic flow speed must start at a specific initial speed from the coronal base, called eigenspeed, go along a continuous eigenfunction, and reach the sonic point, which is where the flow speed equals the sonic speed, while the critical condition, which is where the effective driving force is zero, is satisfied. Any mismatch between the sonic point and critical condition distances results in either subsonic winds when the initial speed is below the eigenspeed, or no stellar wind when the initial speed is above the eigenspeed. Because the critical condition is determined by the stellar wind temperature profile, which depends on ionization process at the top of the chromosphere and the heating process around the coronal base but not by the processes at the sonic point, the required match between the two is generally not met and hence the momentum equation in the conventional theory encounters difficulty when the initial speed is above the eigenspeed. To resolve the difficulty, we propose a discontinuity between the sonic point and the critical condition to reach supersonic stellar wind solutions. As a result, supersonic stellar winds can be produced when the initial speed in the coronal base is greater than the eigenspeed. The critical solution or eigen function provided by the conventional stellar wind model describes the condition that separates the supersonic stellar winds from subsonic ones.

## 1. Introduction

One of the fundamental problems in solar physics is the formation of the supersonic solar wind. The conventional solar wind theory (Parker 1958, 1964a, b, 1965a, b), Figure 1, starts from the coronal base of a million-degree temperature. This leaves the question of how the million-degree temperature can be raised from a few thousand-degree chromosphere (e.g., Klimchuk 2006). Recently, a series of investigations (Song & Vasyliunas 2011; Tu & Song 2013; Song 2017) have shown semi-quantitatively that upward propagating Alfvénic perturbations from the photosphere can be efficiently damped by neutral-plasma collisions in the chromosphere to provide most of the required heat energy for the radiative losses which keep the chromosphere weakly ionized at lower temperatures. Song et al. (2023) further investigated the ionization of the chromospheric gases in the transition region which produces the nearly fully ionized outflow into the corona forming the solar wind. They showed that to produce the fully ionized solar wind flux

observed at the Earth’s orbit, coronal heat sources other than dissipation of the heat flux are needed. Here we recall that although the heat sources in the corona have been widely recognized and agreed upon (e.g., Parker 1960, 1964a, b, 1965a; Hundhausen 1972; Withbroe & Noyes 1977; Aschwanden 2005; Zank et al. 2021), some models suggested that dissipation of downward conduction flux from the corona be sufficient to heat the medium and to launch the solar wind (e.g., Hundhausen, 1972).

The eventual solar wind properties, such as the mass flux and energy flux, depend critically on two processes: the ionization in the transition region, which determines the available mass flux for the solar wind, and the coronal heating around the coronal base which determines the total energy of the solar wind. These two processes cannot be solely determined by processes (or requirements) at the critical point as assumed in the conventional theory, according to which a specific initial flow speed at the inner boundary, called the eigenspeed  $V_e$ , determines whether supersonic solar wind can form or not. This specific initial speed, (see point A in Figure 1), on the other hand, is dictated by the requirement at the critical point. The eigenspeed connects with and crosses the critical point at radius  $r_c$  along a smooth function, which is called the eigenfunction, line A-B in Figure 1. If the solar wind speed generated in the transition region and/or the temperature produced by the heating in the corona does not satisfy the requirement at the critical point, supersonic solar wind cannot form.

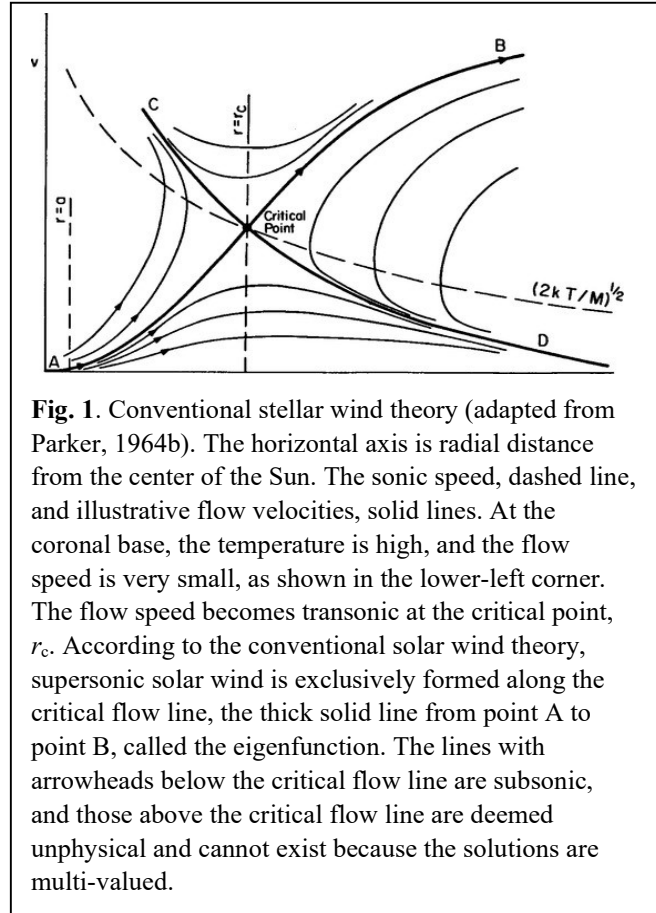


**Fig. 1.** Conventional stellar wind theory (adapted from Parker, 1964b). The horizontal axis is radial distance from the center of the Sun. The sonic speed, dashed line, and illustrative flow velocities, solid lines. At the coronal base, the temperature is high, and the flow speed is very small, as shown in the lower-left corner. The flow speed becomes transonic at the critical point,  $r_c$ . According to the conventional solar wind theory, supersonic solar wind is exclusively formed along the critical flow line, the thick solid line from point A to point B, called the eigenfunction. The lines with arrowheads below the critical flow line are subsonic, and those above the critical flow line are deemed unphysical and cannot exist because the solutions are multi-valued.

The analysis of the formation of the transition region (Song et al., 2023) raised a new question about the validity of the conventional theory. Since the solar wind flux and hence the initial speed at the bottom of the corona is determined by the ionization processes in the transition region, the initial speed may not always equal the eigenspeed but the supersonic solar wind has been observed almost all the time, the conventional model of the formation of the supersonic solar wind needs to be modified or revised. The theory we propose is more generally applicable to the conditions at a variety of stars, and hence, is referred to as a stellar wind theory. However, to demonstrate validity and for quantitative control, we use observed average parameters from the solar chromosphere, coronal base, and solar wind to guide our discussion and semi-quantitative evaluations. Recent observations from the Parker Solar Probe and Solar Orbiter may

provide more constraints on the details for further model development (e.g., Shi et al. 2022; Telloni et al. 2023; Raouafi et al. 2023).

In section 2 we present the one-dimensional steady-state governing equations used in studying the space above the transition region with a focus on the solutions around the sonic point. In section 3, we propose a model of the supersonic wind formation with a discontinuity at the transonic point. In section 4, we show numerical solutions from the model for a range of initial speeds. In section 5, we discuss some concepts in our theory and possible alternatives.

This study concerns a classical problem that has been extensively studied for more than six decades. The conventional theory we refer to in this paper is the fundamental theoretical framework originally proposed by Parker (e.g., Parker, 1958, 1965b; Leer and Holzer, 1980) and does not include those “realistic models” developed in recent years. If the foundation of the supersonic wind formation is modified, these realistic models will need to be modified accordingly. Since this is the first step to fundamentally modify the conventional theory to provide a more solid foundation for further “realistic” and application model developments, we start from the simplest situation of a single-fluid, one-dimensional, steady-state hydrodynamic fluid with generic *ad hoc* heating sources and heat conduction. We leave the inclusion of other effects in the formation of the stellar coronal base and stellar wind, such as asymmetry, multi-dimensionality, non-steady state, electromagnetic field, and specific heating mechanisms for following studies.

## 2. Theoretical Framework

### 2.1 Governing Equations

For simplicity, we consider 1-D radial gas flowing out from a star; at radial distance  $r$  from the center of the star, the number density is  $N$ , and the flow speed is  $V$ . The steady-state governing equations are as follows.

Continuity

$$\frac{\partial}{r^2 \partial r} (r^2 NV) = 0 \quad (1)$$

Since we assume no source or sink (no ionization nor recombination) of the fluid, equation (1) is applicable to regions above the transition region where the fluid is fully ionized.

Momentum equation

$$\rho V \frac{\partial V}{\partial r} = -2 \frac{\partial p}{\partial r} - \rho g + (\mathbf{J} \times \mathbf{B}) \cdot \hat{\mathbf{r}} \quad (2)$$

Here  $2p=(p_i+p_e)$  is the thermal pressure of the plasma, in which factor 2 is a conventional single fluid treatment of electron-ion fluids assuming that the ion pressure equals the electron pressure,  $\rho=mN$  is the mass density,  $m$  is the mass of an ion particle, and  $g = \frac{g_s r_s^2}{r^2} = -\nabla\Psi$  is the gravitational acceleration, where subscript  $s$  denotes the value at the stellar surface, i.e.,  $r=r_s$ . Vectors  $\mathbf{J}$  and  $\mathbf{B}$  are the electric current density and magnetic field, respectively, and  $\hat{\mathbf{r}}$  is the unit vector in the radial direction. When the magnetic field is dominated by the radial component, the  $\mathbf{J} \times \mathbf{B}$  force in the radial direction is negligible.

The steady-state energy equation (e.g., Rossi & Olbert 1970) of the corona, when including cooling (e.g., Vasyliūnas & Song 2005; Song 2017), is

$$\nabla \cdot \left[ \mathbf{V} \left( \frac{1}{2} \rho V^2 + 5p + \rho \Psi \right) + \mathbf{q} + \mathbf{S} \right] = -C \quad (3)$$

where  $\Psi = -\frac{g_s r_s^2}{r}$  is the gravitational potential of the star, and we have assumed the ratio of specific heats to be 5/3 in the thermal energy density. Vector  $\mathbf{S} = \mathbf{E} \times \mathbf{B}$  is the Poynting vector,  $\mathbf{E}$  is the electric field,  $\mathbf{q}$  is the conduction heat flux, and  $C$  is the radiative cooling rate which is not commonly included in MHD theory. We assume that in the corona and the stellar wind, radiation is a pure loss of energy when it is not reabsorbed. The radial component of the Poynting vector is  $S_r = \frac{V B_t^2}{\mu_0} = V \rho c_{At}^2$  where  $B_t$  is the magnetic field component transverse to the flow direction,  $c_{At}^2 = \frac{B_t^2}{\mu_0 \rho}$  is the square of the Alfvén velocity based on the transverse component of the magnetic field, and  $\mu_0$  is the permeability of the vacuum. Although we do not treat electromagnetic effects in this study, we include it here for potential heating sources to be discussed below.

The quantity in the inner parenthesis of equation (3) is the sum of the kinetic, enthalpy, and gravitational potential energy fluxes of the flow. Heating rate  $Q$  can be derived from dissipative MHD and HD processes, which convert the fluid and EM energies to heat (e.g., Song & Vasyliūnas 2011)

$$\nabla \cdot \mathbf{S}_{diss} + \nabla \cdot \left[ \mathbf{V} \left( \frac{1}{2} \rho V^2 + 5p + \rho \Psi \right) \right]_{diss} = -Q \quad (4)$$

Here we emphasize that one cannot simply add the heating rate from a perceived mechanism to the right-hand-side of equation (3). All heating mechanisms have to be derived according to first principles from equation (4) and semi-quantitatively constrained by observations (e.g., Song & Vasyliūnas 2011).

The heat generated by the dissipative processes will be redistributed by the heat conduction flux that flows away from the heating sources according to Fourier's law,  $\mathbf{q} = -\kappa \nabla T$  where  $T$  is the temperature of the plasma and  $\kappa$  is the heat conductivity. If there are no collisions, the divergence of the heat flux  $\nabla \cdot \mathbf{q}_{non}$  is zero. The dissipation of the heat conduction in our problem of a dissipative collisional plasma flow is dominated by electron collisions that produce the divergence of the heat flux  $\nabla \cdot \mathbf{q}_d$ , where  $\mathbf{q}_d = -\kappa_0 T^{5/2} \nabla T$  with  $\kappa_0 = 9.2 \times 10^{-7}$  in CGS units (Spitzer 1956; Aschwanden 2005). Constant  $\kappa_0$  is smaller than that used in other studies (Parker 1964b; Hundhausen 1972; Holzer & Leer 1980). Therefore, the divergence of the heat flux is

$$\nabla \cdot \mathbf{q} = \nabla \cdot \mathbf{q}_d \quad (5)$$

It is worth mentioning that the dissipation of the heat flux, equation (5), is not directly related to the heating mechanisms ( $Q$  in equation (4)). Conductive heating models assumed  $Q=0$ .

In this study, we neglect the convective DC electromagnetic energy, i.e., the DC Poynting vector, and combine dissipative MHD and HD effects as a heating source with an *ad hoc* heating rate  $Q$ .

In 1-D, energy equation (3), combined with equation (1), i.e.,  $r^2 F = r_s^2 F_s$  where  $F = NV$  is the number flux per unit cross-section area and in a single fluid treatment with  $p = NkT$ , where  $k$  is the Boltzmann constant, becomes

$$F_s r_s^2 \frac{d}{r^2 dr} \left[ \frac{1}{2} mV^2 + 5kT + m\Psi \right]_{non} + \frac{d(r^2 q_d)}{r^2 dr} = Q - C \quad (6)$$

Subscript *non* will be dropped from now on for simplicity. The outflowing plasma flux  $F_s$  from the star is primarily determined by the ionization/recombination process in the transition region (see Appendix A).

The physical meaning of equation (6) is clear. The quantity in the brackets is the sum of the fluxes of “non-dissipative” kinetic energy, enthalpy, and gravitational energy that an average particle carries.  $Q$  and  $C$  are the local heat source and sink, respectively, of the energy flux of the medium. The energy from sources or to sinks is redistributed in the flow by heat conduction with (in the presence of dissipation) or without (in the absence of dissipation) conductive heating. Note that there is a possibility of  $\nabla T \neq 0$  while  $\nabla \cdot \mathbf{q} = 0$ , namely, there is a temperature gradient and hence nonzero heat flux, but the dissipation is negligibly small. This is a situation where the heat flux supports the long-range energy redistribution as discussed later in section 3.2. We note that equation (6) is the same as the energy equation of Parker (1964b) when  $Q - C = 0$ . In other words, in Parker’s model, there is no heating other than the dissipation of the conduction flux as we mentioned in the introduction.

In our treatment, there is an *ad hoc* heating source term, similar to that of Leer and Holzer (1980), due to dissipative processes in addition to the dissipation of the heat flux. Heat conduction transfers the heat energy to areas both upward and downward from the heating source. The dissipation of the heat flux converts the heat into other forms of flow energy as a result of collisions. Although we do not specify the mechanism of the additional heating source, many mechanisms from previous theoretical investigations, such as shock heating, cyclotron resonance, kinetic Alfvén waves, resistive heating, and reconnection (see Aschwanden 2005; Zank et al. 2021), have provided a large range of heating rates. For example, the generation and growth of perturbations may draw energy from the flow energy and/or electromagnetic energy (Zank et al. 2021). Nevertheless, we should point out that although most of these mechanisms may not be able to produce enough heating to support the chromospheric radiative losses, they are most likely able to provide sufficient energy for the formation of the coronal base and supersonic stellar wind, which, other than neutral-ion collisions, may be only a few percent of the total required “coronal heating” as discussed before (e.g., Song & Vasyliūnas 2011). In section 4, we assume the *ad hoc*  $Q - C$  term to have the form of a Maxwellian function.

We integrate equation (6) from the lower boundary of the present model,  $r_0$ , to  $r$  and obtain

$$F_s \left[ \frac{m}{2} V^2 + 5kT + m\Psi \right]_{r_0}^r - \left[ \kappa_0 T^{\frac{5}{2}} \frac{r^2}{r_s^2} \frac{dT}{dr} \right]_{r_0}^r = \int_{r_0}^r \frac{r^2}{r_s^2} (Q - C) dr \quad (7)$$

Let

$$E_r = \left[ \frac{m}{2} V^2 + 5kT + m\Psi \right] \quad (8)$$

$$q_r = -\kappa_0 T^{\frac{5}{2}} \frac{dT}{dr} \quad (9)$$

$$H_r = \int_{r_0}^r \frac{r^2}{r_s^2} (Q - C) dr \quad (10)$$

Equation (7) can then be rewritten as

$$F_s E_r + \frac{r^2}{r_s^2} q_r - H_r = F_s E_0 + \frac{r_0^2}{r_s^2} q_0 - H_0 = U_0 \quad (11)$$

where  $U_0$  is the first integral of the energy equation and can be determined at the lower boundary, and subscript  $r$  denotes values at radius  $r$ .  $H_0 = 0$  when  $r=r_0$  from equation (10).

## 2.2 Equations for Stellar Wind Temperature and Velocity

Beyond the coronal heating source region, the net heating rate  $H_r$  from equation (10) reaches a constant  $H_m$  so that  $H = H_m + U_0$  becomes constant, and the energy equation is

$$F_s E_r + \frac{r^2}{r_s^2} q_r = H \quad (12)$$

From the definition of  $q_r$ , equation (9), we then have

$$\frac{dT}{dr} = \frac{F_s E_r - H}{\kappa_0 T^{\frac{5}{2}}} \frac{r_s^2}{r^2} = \frac{1}{\kappa_0 T^{\frac{5}{2}}} \left\{ F_s \left[ \frac{m}{2} V^2 + 5kT + m\Psi \right] - H \right\} \left( \frac{r_s}{r} \right)^2, \quad (13)$$

which specifies the temperature gradient and hence the temperature profile. In steady state, by combining equations (1) and (2) to remove the density, we derive the stellar wind evolution, or momentum, equation (Parker 1958, 1964b; Chamberlain 1961)

$$\left( 1 - \frac{c^2}{v^2} \right) V \frac{dV}{dr} = \left( \frac{2c^2}{r} \right) - \frac{dc^2}{dr} + \frac{\Psi}{r} \quad (14)$$

Here  $c^2 = \frac{2kT}{m}$  is the characteristic thermal speed, and, in the following discussion, is referred to as the sonic speed. Since the sonic speed and the temperature can be directly converted, we use them interchangeably in our equations and discussions, as used in the conventional theory. Equation (14) may be written in a simple form, for later discussions, as

$$L \frac{dV}{dr} = R \quad (15)$$

$$\text{where } L = \left( 1 - \frac{c^2}{v^2} \right) V \quad (16)$$

$$\text{and } R = \left( \frac{2c^2}{r} \right) - \frac{dc^2}{dr} + \frac{\Psi}{r} \quad (17)$$

Substituting energy equation (13) into equation (17) yields

$$R = \left( \frac{4kT}{mr} \right) - g_s r_s \frac{r_s}{r^2} + \frac{2k}{m\kappa_0 T^{\frac{5}{2}}} \frac{r_s^2}{r^2} [H - F_s E_r] \quad (18)$$

As will be shown in subsection 5.1, the physical meaning of  $R$  is the effective driving force. Equation (18) shows that  $R$  is not a strong function of flow speed when the flow is subsonic. In particular, it is not necessarily equal to zero at the distance where the sonic point is approached,

because in general  $R$  depends on the flux from the transition region  $F_s$  and the heating process  $H$ . However, at the sonic point,  $V=c$  and  $L=0$ , so equation (15) becomes

$$0 = R \quad (19)$$

One can easily derive equation (19) from the original form of the continuity and momentum equations when  $V=c$ . Therefore, equations (15) and (19) can be combined as

$$\begin{cases} L \frac{dV}{dr} - R = 0 & (V \neq c) \\ R = 0 & (V = c) \end{cases} \quad (20)$$

Equation (20) is the momentum equation combined with mass conservation. In principle, given the energy flux from the lower boundary,  $F_0 = F_s \frac{r_s^2}{r_0^2}$  and the heating source above the coronal base  $H$ , the stellar wind velocity and temperature as functions of radial distance can be derived uniquely. Whether the solution is continuous or not depends on whether  $R=0$  or not as the sonic point is first encountered.

The conventional stellar wind theory treats the singularity at  $V=c$  as a critical point, that is

$$\frac{dV}{dr} = R/L \quad (21)$$

At the critical distance  $r_c$ ,  $R=0$  and  $L=0$ . The condition  $R=0$  will be referred to as the critical condition while the condition  $L=0$  is the sonic condition. Although the situation for the critical condition and sonic condition occurring at the same point seems reasonable when the singularity is removed and  $V$  and  $T$  remain continuous functions, it is possible that the sonic condition  $L=0$  is reached while  $R$ , defined by equation (18), at  $r_c$  is not equal to zero because  $R$  depends on the flux from the transition region  $F_s$  and the heating process  $H$ . Specifically, if  $R < 0$  at the sonic point, no stellar wind solution can be found from equation (21). This creates a difficulty in the conventional stellar wind theory and is the central issue to be resolved in this study.

### 2.3 Approaching the Sonic Point

From equation (20), close to the star in the parameter range of interest, both  $L$  and  $R$  are negative and increase monotonically with distance. However, since  $L$  and  $R$  are determined differently by the energy and heat fluxes at the lower boundary of the corona and the heating processes around the coronal base, in general, the sonic condition and critical condition do not necessarily occur at the same point. As shown in Table 1, there are three possibilities when the flow reaches the characteristic distance  $r_1$ , this being the radial distance at which either  $L$  or  $R$  first becomes zero in the outflow, with the other parameter remaining negative. The differing cases relate to whether the sonic condition or the critical condition occurs first at the characteristic distance  $r_1$ .

**Table 1.** Three possible scenarios at the characteristic distance  $r_1$ .

	Upstream of $r_1$ $r=r_1^-$		Downstream of $r_1$ $r=r_1^+$		Stellar Wind @ $r \gg r_1$
Only the critical condition is reached No sonic point	$L_1 < 0$	$R_1 = 0$	$L'_1 < 0$	$R'_1 > 0$	Subsonic: $V' < c'$

Parker's and Chamberlain's subsonic solution	$V < c$		$V' < c'$	$T'$ and $V'$ Continuity	$dV'/dr < 0$ $dT'/dr < 0$
Critical condition at sonic point Parker's model	$L_1 = 0^-$ $V < c$	$R_1 = 0^-$	$L'_1 = 0^+$ $V' > c'$	$R'_1 = 0^+$ $T'$ and $V'$ Continuity	Supersonic: $V' > c'$ $dV'/dr > 0$ $dT'/dr < 0$
Sonic point before critical condition Present study	$L_1 = 0^-$ $V < c$	$R_1 < 0$	$L'_1 = 0^+$ $V' > c'$ $\Delta T > 0,$ $\Delta V > 0$	$R'_1 = 0^+$ $T'$ and $V'$ Discontinuity	Supersonic: $V' > c'$ $dV'/dr > 0$ $dT'/dr < 0$

If the critical condition is reached at  $r_1$ ,  $R_1=0$ , before  $L$  reaches zero, then  $L_1 < 0$  downstream of point  $r_1$ , where subscript 1 denotes the value at  $r_1$ .  $R$  then becomes positive while  $L < 0$ , and hence, from equation (20),  $dV/dr < 0$ . The flow thus decelerates and the sonic point  $L = 0$  will never be reached. This, shown as the first scenario in Table 1, gives the subsonic wind solution, corresponding to curves in the area below A- $r_c$ -D in Figure 1, as agreed upon by both Parker and Chamberlain (e.g., Parker 1965b).

The scenario shown in the second row in Table 1 occurs when the sonic condition and critical condition occur at the same point, e.g., equation (21) that *requires*  $R_1=0$  when  $L_1=0$  and is consistent with Parker's supersonic stellar wind solution. We have referred to this scenario as conventional stellar wind theory or the "eigenfunction solution", where the common point is the "critical point". The corresponding initial velocity at the inner boundary is referred to as the eigenspeed,  $V_e$ . At the critical point, this is then a L'Hospital's problem in which the singular point is removable, and the solution for the velocity passes through the critical point smoothly and satisfies the momentum equation (20). The stellar wind becomes supersonic beyond the critical point. Since the supersonic solar wind has been continuously observed, this scenario has been widely accepted to explain *all* solar winds observed in interplanetary space and at the Earth's orbit. As a result, it is believed that *all* supersonic solar winds and hence supersonic stellar winds come along the eigenfunction, line A-B in Figure 1.

Chamberlain disputed this scenario and hence the possibility of supersonic stellar wind because the required initial velocity at the inner boundary, i.e. the eigenspeed,  $V_e$ , allows too small a range of initial velocity to be significant, or as Cranmer & Winebarger (2019) have written "It seemed unlikely that the system would naturally choose this one critical solution out of an essentially infinite number of others that do not become supersonic (see, e.g., Chamberlain 1961)". As shown by equation (18), for a given initial speed, a slight difference in plasma flux  $F_s$  or in net heating rate  $H$  would make the solution of the velocity miss the critical point, so that the solution is either subsonic or there is no numerical result possible beyond  $r_1$ . To address this concern, the stability of the critical point has later been investigated as a solution to this serious problem (e.g., Parker 1966b). Therefore, one may question whether the observation of a



supersonic solar wind can be used as evidence to *exclude* pathways from the inner boundary to interplanetary space *other* than that along the eigenfunction, line A-B in Figure 1.

Parker dismissed the possibility of solutions when  $R_1 < 0$  and  $L_1 = 0$ , shown in the lower row of Table 1. This corresponds to the situation when the initial speed  $V_0$  is greater than  $V_e$ , or curves in the area between A- $r_c$ -C in Figure 1. When the initial speed is greater than the eigenspeed, the flow reaches the sonic point before the critical condition when the effective driving force is still negative and dominated by the negative gravitation potential term in equation (17). Equation (15) is no longer valid because the left-hand-side is zero, but the right-hand-side is not zero. This situation and hence these solutions are unphysical, as Parker argued, because there are two possible values for the velocity at a given distance  $r < r_1$ . This has indeed been shown by Parker and many others for the case of isothermal situations (e.g., Aschwanden 2005; Shi et al. 2023). In the isothermal case, i.e., when equation (13) or the last term in equation (18) is zero, the conventional stellar wind theory relies on the presence of two, not one, intercepting separatrices, A-B and C-D in Figure 1, to argue against supersonic solutions in the area between A- $r_c$ -C. However, in the isothermal case, the sonic speed line is horizontal, and not tilted as in Figure 1 and the total energy is not conserved without continuous heating sources. More generally, with a decreasing temperature profile in equation (13) or an increasing last term in equation (18), the sonic line, the dashed curve in Figure 1, may not intercept with the two separatrices at the same point as shown in Figure 1. Therefore, the existence of the separatrix segment C- $r_c$  is questionable. Without the segment C- $r_c$ , it is possible to directly connect the two regimes above the eigenfunction line A-B.

Nevertheless, because the profiles of  $L$  and  $R$  are determined by the properties of the outflowing plasma flux from the chromosphere, the heating process in the corona, and heat conduction, the situation when  $L_1 = 0$  and  $R_1 < 0$  cannot be dismissed simply because no continuous solution can be found in the previous analyses. This describes our motivation to express the momentum equation in equation (20). It is possible to have a discontinuous solution between the subsonic and supersonic regimes. In the next, we investigate a scenario in which an outgoing supersonic stellar wind can form over a broader range of initial speeds.

### 3. Formation of a Discontinuity at the Sonic Point

#### 3.1 Discontinuity Jump Relations

Based on the above discussion, we propose a discontinuity at the sonic transition for the scenario Parker dismissed. The internal structure of discontinuity cannot be described in detail in our fluid treatment. Across the discontinuity, mass flux, momentum, and energy flux have to be conserved. Since equation (20) is derived from mass conservation (1) and momentum conservation (2), we examine its jump condition. For inner boundary conditions that result in a velocity profile above the eigenfunction, the effective force  $R$  is negative when the sonic point is approached. However, at the sonic point, from the second expression of equation (20),  $R=0$ , there is a jump in the effective force from  $R_1 < 0$  to  $R'_1 = 0$ . Here we follow the tradition by adding a prime to denote the downstream value. The change in the momentum equals the change in the effective driving force,  $R'_1 - R_1$ . From equation (17), we have

$$R'_1 - R_1 = \left(\frac{2c_1'^2}{r_1}\right) - \left(\frac{2c_1^2}{r_1}\right) - \frac{dc_1'^2}{dr} + \frac{dc_1^2}{dr} \quad (22)$$

Not only does the temperature change, but also its gradient. The change in the temperature gradient, which is part of the thermal pressure change, is associated with a change in the heating flux from equation (9). The heat flux change can be determined from energy conservation (12),

$$\frac{r_s^2}{r_1^2} F_s \left[ \frac{m}{2} V_1'^2 + 5kT_1' \right] + q_1' = \frac{r_s^2}{r_1^2} F_s \left[ \frac{m}{2} V_1^2 + 5kT_1 \right] + q_1 \quad (23)$$

We should point out that the discontinuity proposed in the present model is not a shock. By definition, a shock, such as the bow shock and interplanetary shocks often discussed in space physics and astrophysics, refers to a type of discontinuity where the flow changes from supersonic to subsonic state.

Since  $R'_1 = 0$  and  $R_1 < 0$ , and since the right-hand-side of equation (22) is dominated by the temperature terms, across the transonic discontinuity the temperature needs to increase,  $\Delta T > 0$ . For a subsonic upstream flow to become a supersonic stellar wind the velocity jump also needs to be positive,  $\Delta V > 0$ , which leads to a negative density jump,  $\Delta N = N'_1 - N_1 < 0$ . Here symbol  $\Delta$  denotes the difference of the downstream value from the upstream one. Similarly, the velocity jump is  $\Delta V = V'_1 - V_1$ , temperature jump is  $\Delta T = T'_1 - T_1$ , and the heat flux difference is  $\Delta q_r = q'_1 - q_1$ .

The heat flux terms in energy flux conservation equation (23), which affects the temperature gradient term in the effective force, make our jump conditions very different from the conventional Rankine-Hugoniot relations which often assume adiabatic or polytropic processes across a discontinuity (e.g., Habbal and Tsinganos, 1983; Velli, 1994). Without dissipation, the heat flux terms cancel out. As shown in equation (22), with positive jumps in the temperature, the discontinuity requires a reduction of the heat flux,  $\Delta q_r < 0$ , to heat up the medium.

The intensity of the discontinuity, the ratio of the downstream to upstream values, depends on how much heat flux is dissipated within the discontinuity which is ultimately determined by the negative value of  $R$  upstream of the discontinuity. The jump conditions and heat flux dissipation within the discontinuity are self-consistently determined by the conservation laws and the requirement of the downstream supersonic flow condition. Since in our discontinuity treatment, there is no spatial scale for the thickness of the sonic transition layer, the rates of heat dissipation and flow energization are inversely proportional to the actual thickness of the discontinuity layer. The detailed structure and processes therein can be resolved by solving the original form, not the integrated form, of the energy equation (6). To gain a better physical understanding of the processes, which may determine the thickness of the discontinuity, within the transonic region, more theoretical and numerical investigations are needed.

### 3.2 Dissipation of Conduction Flux

Although we have assumed that there are no external heating  $Q$  and cooling  $C$  processes above the coronal base in the region we are considering, from equation (6), the conduction flux carries heat energy from the coronal heating source region to regions of lower temperature over a long range. However, heat conduction flux has been a confusing concept in the context of coronal

heating and stellar wind formation (Hollweg, 1976; Holzer and Leer, 1980). We adapt Spitzer's formula given in section 2.2. From equation (5), one can show that if  $T$  drops with distance at  $r^{2/7}$ , the dissipation is zero while heat flux is  $q_r \sim r^{-2}$  and the divergence of the heat flux vanishes. This temperature drop-off rate may be the asymptotic temperature profile at large distances in the heliosphere before encountering the termination shock. We notice that the heliospheric temperature drop-off rate (Maruca et al., 2024), with a slope of power index -0.273, from 4.4 AU to the termination shock appears to be related to this drop-off rate of a power index -0.286. In regions where the temperature drops faster than this rate, the heat flux dissipates and constantly feeds energy into the flow. Before encountering the sonic transition, as the temperature decreases at a fast rate, the acceleration is accomplished with energy from the dissipation of the heat flux and the reduction of enthalpy.

Upstream of the sonic transition, under the conditions for supersonic stellar winds to form, the energy of the flow, which is the term within the brackets in equation (23), is still negative because of the large negative gravitational energy. The outward energy flux from the coronal base is mostly carried by the heat flux. We recall that the function of the discontinuity in the sonic transition is to increase  $R$  from a negative value to 0 as shown in the last scenario of Table 1. From equation (17), there are two apparently opposing possibilities to increase  $R$ , either to raise the temperature  $T$  or to decrease the temperature more rapidly which increases negative temperature gradient  $|dT/dr|$ . Although a more rapid temperature decrease may indeed lead to a supersonic condition, the decrease in the temperature may further reduce the effective force  $R$  making it remain negative. As a result, the flow speed will decrease, and the supersonic state cannot be sustained. Therefore, this possibility is unphysical—further decreasing the temperature and leading to an oscillatory decreasing flow speed around the sonic speed until the temperature unphysically becomes negative.

The remaining possibility would then be a jump in the temperature at the discontinuity. Across the sonic transition, from equation (14),  $L=0^-$ , the velocity increases rapidly. From energy conservation equation (12), the change in the heat flux is

$$-\Delta q_r = \left( \frac{m}{2} \Delta V^2 + 5k\Delta T \right) F_s \left( \frac{r_s}{r} \right)^2 \quad (24)$$

With the increases in temperature and velocity, the heat flux decreases. This produces a discontinuous drop in the heat flux. Since the downstream temperature is higher, the reduced heat flux can be accomplished by a flatter temperature profile further out. In equilibrium, the requirement of the energization of the flow determines self-consistently the amount of heat flux dissipation. Therefore, dissipation of the heat flux is extremely strong within the discontinuity and the heat flux decreases across it. This explains the cause and the location of the discontinuity.

### 3.3 Formation and Stability of the Discontinuity

The formation of a discontinuity first needs a wave steepening process. A well-known wave steepening process is the nonlinear steepening formation of wave fronts, such as in the shallow water wave, but the conventional nonlinear wave steepening process is not applicable in our case. In the corona-solar wind system, neglecting the electromagnetic fields, the perturbations

propagate as sonic waves, propagating both upward and downward and each propagates at sonic speed in frame of reference of the flow. The net perturbation  $dV$  is the summation of the upward and downward propagation. When a perturbation  $dV$  starts from the coronal base and goes upward, one can show that the perturbation follows an equation exactly same as equation (14) by replacing  $dV/dr$  with  $ddV/dr$ . When  $ddV/dr$  is positive (negative), the flow accelerates (decelerates) with distance. For  $R < 0$ , in the subsonic regime, the net perturbation speed gradually increases while the sonic speed decreases as the temperature decreases. At the sonic point, the downward propagation ceases to propagate because the downward propagation is carried back by the upward flow and the perturbation forms a standing wave. The upward perturbation is able to continuously propagate upward.

However, as discussed in subsection 3.2, enhanced dissipation of the heat flux takes place in the sonic transition leading to a higher downstream flow speed and higher temperature which is proportional to the square of the propagation speed. Further out from the discontinuity, the flow speed continues increasing while the temperature and hence the sonic speed decrease. A discontinuity is then formed to separate the subsonic and supersonic regimes.

A stable discontinuity structure requires the process that forms it to be irreversible; otherwise, it will dissolve or disperse easily even after it is formed. Since a process with increasing entropy is irreversible, often an increasing entropy, instead of irreversibility, is used as a proxy for a stable discontinuity/shock jump condition. We then analyze the change in the entropy. In an ideal gas, with added heat from the dissipation of the heat flux  $-\Delta q_r$ , the entropy change is

$$\Delta S = -\Delta q_r / T \quad (25)$$

Combining equations (24) and (25), at the sonic transition, yields

$$\Delta S = \left[ \left( \frac{\Delta V}{c_1} \right)^2 + 5 \frac{\Delta T}{T_1} \right] k F_s \left( \frac{r_s}{r_1} \right)^2 \quad (26)$$

With the accelerated flow  $DV > 0$  and the increased temperature  $DT > 0$ , the entropy increases  $DS > 0$  across the discontinuity. Therefore, the processes that form the discontinuity are irreversible, and the structure of the discontinuity is stable. The stable discontinuity is a rarefaction, which invalidates the over-generalized conception that rarefaction jumps are inadmissible in the Rankine-Hugoniot conditions. This is not because the Rankine-Hugoniot condition failed but because the generalization of it from a specific situation to a more complicated situation is not valid. In our more complicated situation, there is conduction heat flux that is discontinuous across the discontinuity. There is substantial heat added within the discontinuity due to the strong dissipation of the heat flux.

#### 4. Supersonic Stellar Wind Solutions

The supersonic stellar wind temperature and velocity profiles start from the inner boundary conditions at the top of the transition region, assumed to be at  $r_0 = 1 r_s$  (Song et al. 2023). We assume that the *ad hoc* heating function is a normal distribution centered at  $2 r_s$ , with a half-width of  $0.15 r_s$ . Above  $2.5 r_s$ , the heating source,  $Q \approx C \approx 0$ , and the total heating reaches its maximum value  $H_r = H_m$ . The solutions are derived directly from equations (13) and (20). Figure

2 shows solutions for five initial velocities,  $V_0$ , at the lower boundary with other parameters, such as the temperature  $T_0$  at  $r_0$  (Song et al. 2023), heating rate  $H_m$ , density  $N_s$ , and eigenspeed  $V_e$ , held fixed.

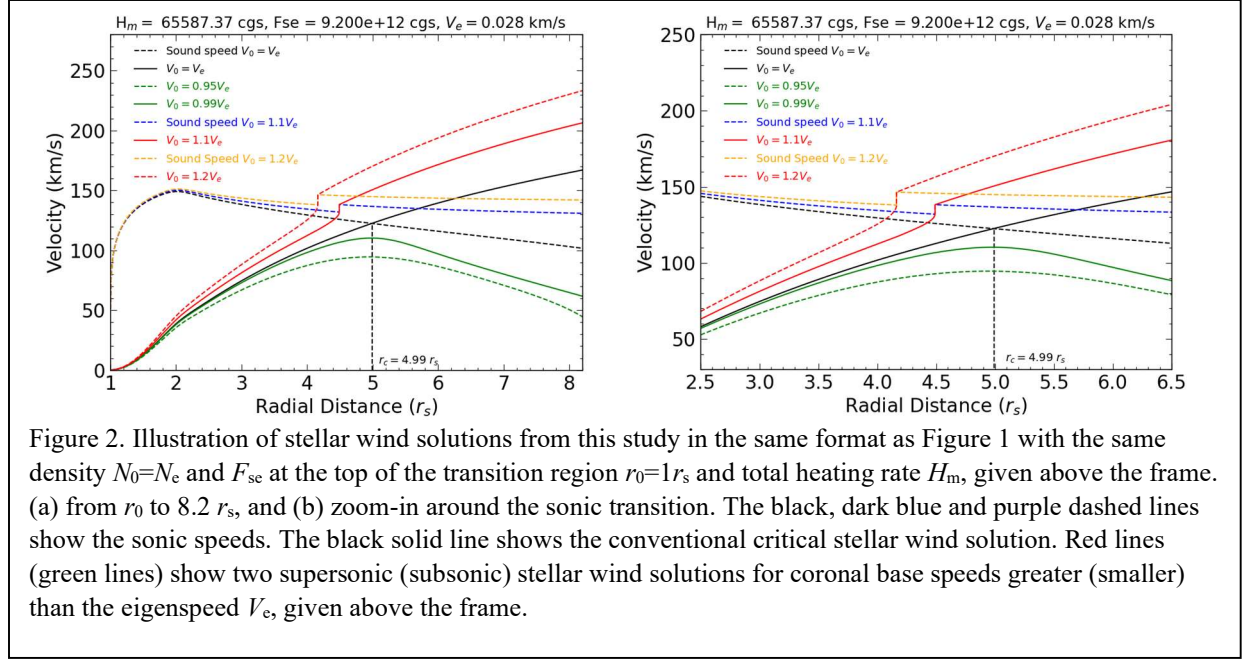
We have tested several standard algorithms to solve these two relatively simple coupled ordinary differential equations and the results are consistent, repeatable, and unambiguous. The location and the energy of the flow are affected by the inner boundary conditions,  $V_0$ ,  $V_e$  and  $F_s$ , and by the location, width, and magnitude of the heating source  $Q$ . We have also tested different spatial step lengths. The step length shown in Figure 2 is 60 km. For the cases with initial speeds greater than the eigenspeed,  $V_0 > V_e$ , the results all unambiguously show that the calculation stops at the sonic point. No solution can be found further. When the step length is large, for example, a fraction of a solar radius, corresponding to the commonly used step length in global corona-solar wind models, the calculation is able to jump over the singularity at the sonic speed, the dashed line in Figure 1. However, we do not show these results because we think the downstream solutions result from large numerical dissipations.

The solid (dashed) black line in Figure 2 shows the flow speed (sonic speed) for the critical/eigenfunction solution,  $V_0 = V_e$ . It is worth mentioning that to derive the critical solution,  $V_e$  has to be extremely accurate—down to the 11<sup>th</sup> digit, which may be correlated to the spatial resolution,  $10^{-4} r_s$ , used in the calculation. Otherwise, the solution is either subsonic or singular. Therefore, the results are consistent with Parker’s theory. Strictly speaking, the only difference is the missing supersonic segment below line C- $r_c$  in Figure 1. However, it also implies that Parker’s critical solution may not be able to provide a meaningful amount of supersonic stellar wind without substantial physical or artificial dissipation. If the spatial resolution is low, say,  $0.1 r_s$ , the critical point condition would not be as acute, and the solutions could step through the critical point with small fluctuations.

We are interested mostly in the supersonic stellar wind. Stellar winds with greater initial speeds, shown by solid and dashed red lines, reach sonic speeds closer to the star. If  $V_0 > V_e$ , the solution stops at  $r_1$  where the sonic point,  $L=0$ , is encountered while  $R < 0$ , as shown in the third scenario in Table 1 where the first expression of equation (20) encounters the singularity. However, the second expression of equation (20) is valid at the singularity. A discontinuity is needed between the two solutions. The quantities from the upstream, including  $R_1$ , are used to determine the values downstream using equations (22) and (23) assuming  $R'_1=0$  and  $L'_1=0$ . Equations (13) and (15) are then used to calculate the temperature and velocity profiles further out.

Parker’s critical solution and the subsonic solutions correspond only to situations for  $R_1 \geq 0$  at the critical distance. The solutions are shown by the green and black lines in Figure 2. For the subsonic solutions (green lines), the solutions diverge rapidly before encountering the critical point when the initial speed is merely slightly smaller (1%) than the eigenspeed. In the subsonic solutions, the total heat flux, which is the heat flux over the whole  $4\pi$  sphere, dominates the energy flux and reaches an asymptote so that the kinetic energy and the enthalpy decrease to provide energy to counter the gravitational potential energy.

The jump condition relations in equations (22) and (23) only relate the upstream and downstream



flow conditions of a discontinuity, but the discontinuity does not necessarily result in a supersonic downstream flow. The supersonic solution is guaranteed by the heating flux effect. From equation (13)  $dT/dr < 0$ ,  $R'$  will increase to  $R' > 0$ . With the decrease of sonic speed,  $L$  increases to become positive,  $L' > 0$ , and then from equation (15),  $dV/dr > 0$ , forming the supersonic stellar wind.

## 5. Discussion

### 5.1 Physical Description of the Formation of a Supersonic Stellar Wind

The physical processes learned from the analysis presented in this study are as follows. In the simple example of a vertical flux tube, an isotropic fluid is driven by two opposite forces: the upward pressure gradient force and downward gravitational force. The pressure gradient force has two contributors, the temperature gradient, and the density gradient. If the flow is compressible, the density gradient results in an opposite flow velocity gradient and a geometric effect associated with the expansion in the cross-section area of the flux tube. The momentum equation, combined with the continuity equation, can be written as

$$mN \frac{VdV}{dr} = mN \frac{c^2}{V} \frac{dV}{dr} + mNR \quad (27)$$

where  $R$ , defined in equations (17) or (18), can now be understood as the effective driving force including the temperature gradient force, gravity, and the expansion effect. The first term on the right of equation (27) is due to the effect of the density gradient. Since the formation of the supersonic stellar wind is essentially a process which increases the kinetic energy, it is clearer to express equation (27) in terms of the change in the kinetic energy flux on the left and the work done on the right, by multiplying equation (27) by  $V$

$$F \frac{d(\frac{mV^2}{2})}{dr} = F \frac{c^2}{v^2} \frac{d(\frac{mV^2}{2})}{dr} + mFR \quad (28)$$

where  $F=NV$  is the number flux. The first term on the right is due to the density decrease which accelerates the flow. Where  $R<0$ , the effective driving force  $R$  does negative work to slow down the expansion of the flow. When  $R>0$ , on the other hand, the effective driving force does work to accelerate the flow in addition to the expansional effect of the density decrease. Therefore, the real flow acceleration starts when  $R=0$ , which is the critical condition.

Physically, if the incoming stellar wind starts with a greater initial speed and reaches sonic speed before reaching the critical condition  $R=0$ , the wind cannot flow faster than the sonic speed. A discontinuity can accomplish the task by making the downstream region satisfy the critical condition for the supersonic stellar wind to form. Therefore, the eigenfunction in Parker’s stellar wind theory is actually the boundary separating the stellar winds that can reach the supersonic condition from those cannot at the transition region. A higher outgoing speed results in a higher stellar wind speed. For speeds less than that of the eigenfunction, the fluid flows more slowly and forms a subsonic wind.

By analogy, in the conventional supersonic stellar wind theory, the critical point functions more like a security guard who allows only the stellar wind with correct IDs, which is the initial speed  $V_0$  at the inner boundary that matches the eigenspeed  $V_e$ , to pass. Numerical tests have shown that the correct ID match has to be exact up to 14 digits which can occur only in an extremely small range,  $\sim 10^{-9}\%$ , depending on the spatial resolution and numerical diffusive/viscous effects. If not matched, the output is either subsonic solutions (pass to slow lanes) or no solution (no pass). This is in support of Chamberlain’s dispute (1961).

## 5.2 Critical Point and Eigenfunction Solution

Conventional supersonic stellar wind theory has been based on the assumption that the singularity in the evolution equation (14) is removable by restricting the inner boundary condition of the system. However, this restriction is so strong that no significant flux of supersonic stellar wind can be produced. Furthermore, a more serious issue is that the inner boundary condition is derived “in reverse” by requiring knowledge of downstream conditions. That is, the required velocity at the inner boundary is mapped back from the critical point several stellar radii away along the eigenfunction, i.e., the line A-B in Figure 1. If the initial velocity cannot satisfy the critical condition at the sonic point, the stellar wind either cannot form physically or has to be subsonic as discussed in section 2.3 and shown in Figure 1. The most problematic conclusion is in the former case—if in reality the initial speed is greater than the eigenspeed, there would be no stellar wind (solution), neither supersonic nor subsonic.

By contrast, in our model, the outflowing flux of corona/stellar wind is determined in the transition region (assumed to be the stellar surface  $r_0=r_s$ ),  $F_s= N_0V_0$ . The stellar wind then flows out without much pre-knowledge about the existence of the critical point.  $T_0$  is determined by the first impact ionization potential (Song et al. 2023), but  $V_0$  cannot be determined without knowing the outflowing flux and density at  $r_0$ . Therefore, there is a potential mismatch between  $V_0$  and the eigenspeed  $V_e$ , a situation when the conventional theory eliminates possible stellar wind

solutions when  $V_0 > V_c$  using the “unphysical” argument. Under this condition, because  $L=0$  and  $R<0$ , the conventional momentum equation (15) is not able to describe the process. We have rewritten the momentum equation as equation (20) by defining the condition at the singularity with the sonic condition  $R=0$  while allowing a discontinuity to connect the two regions. Parker’s critical point condition,  $R=0$  when  $L=0$ , allows only a continuous solution which is only one of the possible solutions to the singularity issue which is valid in a very small parameter range. i.e. it is a singular solution. In the present model, a large range of possible velocities at the inner boundary may be able to pass through the sonic condition and become a supersonic stellar wind.

Stellar atmospheric processes and conditions should determine the properties and locations of the sonic point and critical condition and not be determined by the downstream requirement. What is not apparent in equation (14) in the conventional theory is the absence of the mass flux or density. Although density  $N_0$  can be given at the inner boundary according to mass conservation, the density does not affect the eigenfunction solution in the conventional theory. Parker included the density later in his series of investigations. When including the heat flux, he concluded that there is a critical or eigen density  $N_B$  which may determine whether the stellar wind is supersonic or subsonic (Parker 1965a). That is, when  $N_0 < N_B$  ( $N_0 > N_B$ ), the stellar wind will be supersonic (subsonic). His conclusion is qualitatively consistent with our critical condition scenario in Table 1 since for a given initial flux  $F_s$ , a lower density results in a higher speed.

The present model is based on the thermal conduction formalism and is characteristically different from many stellar wind models that make either an isothermal or polytropic assumption to simplify the energy equation (e.g., Parker 1958; Velli et al. 1994, 2001; Shergelashvili et al. 2020). Here we should point out that the energy conservation equation (11) holds at any reference point above the transition region when the fluid is fully ionized. For example, the reference point can be set above the heating sources. In this case, although there is no active heating, the total heating  $H_0 = H_m$  in equation (11) can be nonzero. In fact, we believe that implicitly dropping  $H_m$ , which represents the heating around the coronal base, in the energy conservation may have led to the energy problem, according to which conventional solar wind models predict lower energy at 1 AU than observed (Holzer 1977; Hundhausen 1982).

The existence of the solar magnetic field will not fundamentally change the transonic solutions discussed here. Unless the sonic transition occurs in the region of active reconnection, the magnetic effect will in principle modify the present theory by replacing sonic speed with the magnetic sonic speed,  $c_{ms}^2 = c^2 + c_{At}^2$ , and hence the sonic point becomes the magnetosonic point. If the magnetosonic speed is much greater than the sonic speed, the sonic transition may be referred to as the Alfvén transition (Wexler et al., 2021).

### 5.3 Time-Dependent Effects and Spatial Oscillation Solutions

It has long been argued that the critical point is a problem occurring only in highly idealized treatments and does not occur in actuality. One may argue, for example, that in a non-steady state process, there is no critical point (e.g., Suess, 1982; Holzer and Leer, 1997). Although the time-dependent theory of the supersonic stellar wind formation deserves several full-length studies, the time-dependent effect alone may not be able to produce supersonic stellar winds. For



example, if the density is not time-varying and flux is conserved, the time dependent momentum equation can be written as

$$\frac{\partial V}{\partial t} + L \frac{\partial V}{\partial r} = R \quad (29)$$

At the sonic point  $L=0$ , for an initial speed greater than the eigenspeed when Parker's theory does not provide a solution,  $R<0$  results in  $\partial V/\partial t < 0$ . Namely, the flow speed can only decrease with time and the supersonic condition cannot be reached or maintained.

Instability analyses of the critical point have been carried out in many studies (e.g., Park, 1965b; Velli, 1994, 2001; Keto, 2020) to argue that the critical point is unstable and hence the critical point cannot stay. Here we recall that an instability analysis studies whether an equilibrium is stable or not and an instability analysis is meaningless if no equilibrium can be found. Therefore, the analysis must start with an equilibrium. However, in the situation of interest, for  $V_0 > V_e$ , equation (15) does not provide such an equilibrium. Therefore, the instability analysis method cannot contribute to addressing the problem that little supersonic stellar wind can be produced in the conventional theory.

In numerical solutions of the transonic models, spatial oscillations are often found starting at the sonic point. These spatial oscillations, in contrast to temporal oscillations, can be understood as follows. We start with a subsonic flow from the star with  $L<0$  and  $R<0$ . From equation (13), in the region where the heating rate  $H$  is sufficiently large in order to produce supersonic stellar winds from the corona (the inner brackets in the second expression),  $T$  decreases. Before  $L$  reaches zero, from equation (15),  $dV/dr > 0$ , so that the flow accelerates to reach  $L=0$ . When the flow speed crosses the sonic point at  $r_1$  and becomes supersonic, from equation (16),  $L > 0$ . If  $R$  remains negative, equation (15) then requires  $dV/dr < 0$ , so that the flow decelerates to become subsonic. Then, since  $L<0$ ,  $dV/dr > 0$ , and the subsonic flow will accelerate to become supersonic again. The same acceleration-deceleration-then-acceleration-deceleration process repeats. In general, this situation thus results in a flow speed that spatially oscillates around the sonic speed. This pattern is similar to that shown in Figure 3d of Holzer (1977) which presented one cycle of the oscillation. The sonic point  $L=0$  in the present model is equivalent to his first saddle point and the critical condition  $R=0$  equivalent to the second saddle point. However, the wavelength of the spatial oscillation would depend on the resolution of a numerical solution. We should point out that without invoking artificial dissipation, the oscillation cannot be damped. A finer resolution would result in more oscillations until the second saddle point,  $R=0$ , is reached.

Rather than explicitly considering the situation in which the velocity oscillates about sonic speed, one may idealize and approximate it as a "sonic layer" through which  $V=c$ . Within this layer, the momentum equation (15) is then replaced by  $V=c$  because equation (15) can no longer describe the situation at  $L=0$  if  $R<0$ , a situation that can occur in reality. Numerical tests have shown that the sonic layer approximation can produce good results in which the momentum across the sonic transition is conserved up to  $10^{-5}$  of the net momentum. However, this approach, although providing very good results, may be considered only as an approximation because one may not be able to prove that the solution within the sonic layer satisfies the momentum equation.

## 5.4 Inevitability of Unremovable Singularity

The proposed discontinuity is needed when the singularity at the sonic point in equation (14) is not removable. One may challenge our model by arguing that the singularity may be always removable. For example, they argue that if neglecting dissipation, and assuming the flow is subsonic at the base, there are only 2 incoming characteristics into the system, a sound wave and an entropy wave. Therefore, only two boundary conditions may be imposed, either density  $N$  and temperature  $T$ , or velocity  $V$  and temperature  $T$ , or density  $N$  and velocity  $V$ . The system will then relax to a stationary state. Now the physically reasonable conditions to impose are  $N$  and  $T$  in the chromosphere.  $V$  will therefore adapt itself to go into the Parker-like critical solution automatically. If you impose  $N$  and  $V$ , on the other hand, then  $T$  will adjust to create the critical solution.

Let us first consider the simple isothermal system analyzed in Parker's original proposal, without the energy equation, with two inner boundary conditions for  $N$  and  $V$ . One can indeed find solutions for  $V$  as a function of  $r$ . However, the solution may stop at the sonic point depending on whether the critical condition  $R=0$  can be reached or not exactly at this point. However, this depends on the temperature  $T$ , an unspecified yet. If  $T$  is smaller than a certain value so that  $R<0$ , no supersonic solution can be found. Similarly in other possible inner boundary conditions as described above. Therefore, the above argument is not true. Theoretically, the argument overlooked the possibility that there are two, not one, sound waves, one propagating outward and one inward. Parker's theory described a solution allowing the flow to return to the sun as shown in Figure 1.

The most important ingredient in our model is the "dissipation" of the heat flux. With the dissipation, the energy conservation equation has to be included. We, therefore, have 3 dependent variables and three equations so that the temperature cannot be "adjusted" at one's wish. We recall that if one employs an isothermal or polytropic assumption,  $T$  is no longer a real dependent variable but a function of  $N$ . With 3 dependent variables, it is more obvious that one cannot guarantee a continuous sonic transition as discussed in the text around equation (19). This is the central issue of our model.

## 5.5 Observation

In this preliminary stage of model development, it may be too early to predict the observational differences between the present model and the conventional one using currently available observations. Nevertheless, we may discuss conceptually the differences between the two models. Let us assume that with the same stellar wind density and temperature, the initial velocity,  $V_0$ , has a range of possible values. Both models would predict that when  $V_0 < V_e$ , the stellar wind is subsonic. The conventional model predicts that all supersonic stellar winds arise with  $V_0 = V_e$ , while speeds with  $V_0 > V_e$  cannot go through the sonic point (because no single-valued mathematical solution can be found). Accordingly, a supersonic stellar wind cannot form easily because most often the theory does not allow a solution. If there is a finite range of distribution in the speed at the inner boundary, only a small amount of the flux will be able to get through. Consequently, a supersonic stellar wind may be observed either only occasionally or with

extremely small average fluxes. By contrast, in the present model, all flow speeds with  $V_0 \geq V_c$  can become supersonic stellar wind. If the initial speed is greater, both the stellar wind speed and the temperature are higher. Therefore, supersonic stellar winds can be continuously observed most of time with large fluxes and a range of variable speeds, temperatures, and densities, as shown in Figure 2. Comparing red/blue/orange lines with black lines on the right side of Figure 2, the solar wind temperature, velocity, and Mach number predicted by the present model may also tend to be higher than that of Parker’s model for the same coronal temperature and Parker’s eigenfunction should correspond to the lower bound of the wind speed.

Recent observational reports from the Parker Solar Probe (Raouafi et al 2023) suggest that although the solar wind speed has a large range variability, there is a possible lower bound for the supersonic solar wind speed as a function of the radial distance. Furthermore, this lower bound has a shape and value similar to that of Parker’s eigenfunction. This observation may be interpreted as to be consistent with the conventional theory; the lower bound may indicate the lower limit of the coronal base temperature, and the range of the velocities above the bound may be explained by the temperature fluctuations in the coronal base. Indeed, if both the temperature and velocity both fluctuate at the coronal base, the solar wind at Park Solar Probe orbits can be observed with temperature and velocity fluctuations. However, according to the conventional theory, at a given time only a small fraction of the flux has the velocity that matches the required critical condition. Therefore, the observed flux should be intermittently and on average much smaller than that available at the coronal base and there should be periods of time when the supersonic solar wind is absent.

By contrast, our model would interpret the observed range of the velocity and temperature result from the varying heating rate in the corona and chromosphere and the lower bound results from the energy bound required for supersonic solar wind described by Parker’s eigenfunction.

## 6. Conclusions

To describe the stellar wind, the evolution of the momentum equation has a singularity at the sonic point where the flow speed equals the sonic speed. In the conventional stellar wind theory, the supersonic stellar wind solution is based on a continuous solution, which requires the critical condition to be satisfied at the sonic point in order to remove the singularity with a continuous function. However, the critical condition and sonic point are in general two independent conditions. We demonstrate that except in extremely rare situations, the two conditions do not occur at the same point and the singularity at the sonic point is not always removable with a continuous function. This is because the critical condition is determined by the upstream conditions for the formation of the stellar wind, i.e., the ionization process that determines the mass flux of the stellar wind and the heating processes around the coronal base that determine the total energy of the stellar wind. Therefore, the conventional stellar wind theory needs fundamental modification or reformulation.

We then revisited the conventional stellar wind theory, especially its line of reasoning. In the conventional stellar wind theory, the requirement for the two conditions to be satisfied at the same point functions more like an ID checkpoint at the sonic point. The problem is that the check

is not about the plasma parameters locally at the sonic point but about the initial velocity at the inner boundary of many stellar radii upstream. By analogy, the ID check is not about the characteristics of the person but about their parents or grandparents. Specifically, if the initial speed is greater than the eigenspeed, according to the conventional theory, the flow is not allowed to pass through the checkpoint with no option of how to go further, the most problematic conclusion of all. We questioned whether the initial speed at the inner boundary should be quantitatively checked at the critical point as the condition for formation of the supersonic stellar wind. Although the properties of the flow close to the sonic point may be influenced and modified by the existence of the transonic condition, there should be no question that the flow will pass across the sonic point either supersonically or subsonically. That no physical solution can be found cannot be used as a reason to stop the flow from forming either a subsonic or supersonic stellar wind at the sonic point simply because its initial speed at the inner boundary is greater than the eigenspeed.

With the insight gained from the processes forming the transition region (Song et al., 2023), the stellar wind plasma flux is controlled primarily by ionization of the neutral particles from the chromosphere over the transition region with the energy primarily from the dissipation of the downward heat flux produced from heating in the coronal base. Therefore, the stellar wind flux is not determined by the critical point condition. When the flow properties are determined by the processes well upstream in the chromosphere, the singularity cannot be removed, and the singular solution provided by the conventional theory is not valid. The inability to find a solution under these conditions when the initial speed is greater than the eigenspeed cannot be used to prevent these possible physical conditions to occur. It may be interpreted as a failure of the expression of the momentum equation (14) at the singular point. A different treatment may be introduced to address the singularity issue. After investigating possible instabilities, possible sonic layer, and time-dependence effects at the critical point, we propose a discontinuous solution.

In our model, the stellar wind energy flux is determined by the heating processes in the corona, and the stellar wind flux is determined by the ionization process from the transition region. The coronal base temperature is a characteristic measure of energy. When encountering the sonic point, depending on the flux and energy, the stellar wind will become either supersonic or subsonic, as predicted by the conventional theory. However, only a negligibly small fraction may pass smoothly across the sonic point along the eigenfunction line A-B in Figure 1 as described by the conventional theory, and most stellar wind will pass through a discontinuity at the sonic point to gain enough energy becoming supersonic, a possibility that has not been considered in the conventional theory. The eigenfunction in the conventional theory is actually the separation line between the supersonic and subsonic stellar wind conditions. The sonic transition problem has not drawn much attention from large-scale numerical modeling, most likely because of the coarse spatial resolution. When the spatial resolution is a fraction of a stellar radius, numerical effects may be large enough to damp the oscillations within the sonic transition layer. In comparison, the spatial resolution shown in this study is  $10^{-4} r_s$ . With the availability of faster computers, the transonic issue is becoming more and more obvious (e.g., Adhikari et al. 2022).

The detailed physical processes within the discontinuity need further theoretical and numerical investigations.

## Appendix A: Formation of Stellar Wind Plasma Flux

Because the chromospheric density is high and the temperature is low, most of the energy from chromospheric heating is lost to radiation when the temperature is below the first impact ionization potential of dominant species and the ionization fraction is low. If, on the other hand, the heat source is up in the corona, ionization can take place more efficiently on the top surface of the chromosphere, i.e., the transition region, by dissipation of the downward heat flux in a process similar to sunlight evaporating a moist land surface. Heating, ionization, and radiative losses in the chromosphere and transition region have been investigated (Song and Vasyliunas 2011; Song 2017; Song et al. 2023).

The temperature at the top boundary of the transition region may be determined by the first impact ionization potential  $\Phi_i$  of dominant species there, which corresponds to  $T_{ts} \sim 158\text{kK}$  for hydrogen. Based on the Song et al. (2023) model, the transition region is formed from weakly ionized gas to fully ionized plasma with the heating mostly arising from conversion of the coronal heat conduction flux and cooling from the energy losses due to radiation and ionization. This is where the ionization fraction increases from 0.5 to 1.0. The net ionized plasma flux is, from equation (20) of Song et al. (2023),

$$F_s = \frac{-\Delta q_{ts} + (Q_{ts} - C_{ts})\Delta r_{ts}}{0.5\Phi_i + \Delta E_{ts}} \quad (\text{A1})$$

where subscript  $ts$  denotes the value at the top boundary of the transition region,  $\Delta r_{ts}$  is the thickness of the stellar transition region,  $\Delta q_{ts}$  is conduction flux dissipated in the transition region and may be similar to that from the corona flowing into the transition region,  $Q_{ts}$  is the net heating rate,  $C_{ts}$  is the radiative cooling rate, and  $\Delta E_{ts} \sim 5kT_{ts}$  is the energization in the transition region from the chromosphere. To the lowest order, the ionized stellar wind energy flux is produced by a small fraction of the conduction flux from the corona,  $q_{ts}$ , but a significant part of the heat flux is radiated away by  $C_{ts}$ . Since the radiative cooling is approximately proportional to the square of the density, the stellar wind flux is, though not explicitly expressed, a strong function of the density which is determined by the properties of the star. At the top of the solar transition region, i.e., the lower boundary of solar corona, the density is  $N_{ts} \sim 2.95 \times 10^9 \text{ cm}^{-3}$  and the velocity is  $V_{ts} \sim 3.1 \times 10^3 \text{ cm/s}$ , giving the number flux  $F_s \sim 10^{13} \text{ cm}^{-2} \text{ s}^{-1}$ , in the same range as the solar wind flux observed at the Earth's orbit (Hundhausen 1972).

## Acknowledgments

We thank Drs. V. M. Vasyliunas, M. G. Kivelson, and G. P. Zank for their valuable comments and suggestions.

## References

Adhikari L., Zank G. P., Telloni D. et al. 2022 *ApJL* **937** L29

- Aschwanden, M. 2005 *Physics of the Solar Corona: An Introduction with Problems and Solutions* (New York: Springer)
- Chamberlain J. W. 1961 *ApJ* **133** 675
- Cranmer S. R. and Winebarger A. R. 2019 *Ann. Rev. Astron. Astrophys.* **57** 157
- Habbal S. R. and Tsinganos K. 1983 *J. Geophys. Res.*, **88** 1965
- Hollweg, J. V. 1976 *J. Geophys. Res.*, **81**, 1649,
- Holzer T. 1977 *J. Geophys. Res.* **82** 23
- Holzer T. E. and Leer E. 1980 *J. Geophys. Res.* **85** 4665
- Holzer, T.E., Leer, E. 1997 *Fifth SOHO Workshop: The Corona and Solar Wind Near Minimum Activity*, A. Wilson (ed.), 404, ESA, Noordwijk, 65.
- Hundhausen A. J. 1972 *Coronal Expansion and Solar Wind* (New York:Springer)
- Keto, E. 2020, *Mon. Not. Roy. Astron. Soc.* 493, 2834.
- Klimchuk J. A. 2006 *Solar Phys.* **234** 41
- Parker E. N. 1958 *ApJ* **128** 664
- Parker E. N. 1960 *ApJ* **132** 821
- Parker E. N. 1964a *ApJ* **139** 72
- Parker E. N. 1964b *ApJ* **139** 93
- Parker E. N. 1965a *ApJ.* **141** 1463
- Parker E. N. 1965b *Space Sci. Rev.* **4** 666
- Parker E. N. 1966 *ApJ* **143** 32
- Raouafi N. E., Stenhorg G., Seaton D. B. et al. 2023 *ApJ* **945** 28
- Rossi, B. and S. Olbert 1970 *Introduction to the Physics of Space* (New York: McGraw-Hill)
- Shergelashvili B. M., Melnik V. N., Dididze G., et al. 2020 *MNRAS* **496** 1023
- Shi C., Velli M. Bale S. D. Réville V. et al. 2022 *Phys. Plasmas* **29**, 122901
- Song P. and Vasyliūnas V. M. 2011 *J. Geophys. Res.* **116** A09104
- Song, P. 2017 *ApJ* **846** 92
- Song P., Tu J., Wexler D. B. 2023 *ApJL* **948** L4
- Spitzer L. Jr. 1956 *Physics of Fully Ionized Gases* (New York: Interscience)
- Suess, S.T. 1982, *ApJ.* 259, 880
- Telloni D., Romoli M., Velli M., et al. 2023 *ApJ.* **954** 108 doi:10.3847/1538-4357/aceb64
- Tu J. and Song P. 2013 *ApJ* **777** 53
- Vasyliūnas V. M. and Song P. 2005 *J. Geophys. Res.* **110** A02301
- Velli, M. 1994 *ApJL* **432** L55

Velli, M. 2001 *Astro. Space Sci.* **277** 157

Wexler D. B., Stevens M. L., Case A. W. and Song P. 2021 *ApJL*. **919** L33

Withbroe G. L. and Noyes R. W. 1977 *Ann. Rev. Astron. Astrophys* **15** 363

Zank G. P., Zhao L. L., Adhikari L. et al. 2021 *Phys. Plasma* **28** 080501